

## Intrinsic ductility criterion for interfaces in solids

Robb Thomson

*Materials Science and Engineering Laboratory, National Institute of Standards and Technology,  
Gaithersburg, Maryland 20899*

(Received 3 April 1995)

This paper explores the cleavage vs blunting dislocation emission from a crack on an interface in a two-dimensional simple hexagonal lattice for a variety of nearest-neighbor central force laws, and compares the results with elastic predictions of the criteria couched in terms of the interfacial surface energy,  $\gamma_s$ , and the unstable stacking fault,  $\gamma_{us}$ . The mode conversion characteristic of interfacial cracks is interpreted in terms of a local phase at the core of the crack, with a cutoff at the force law range parameter. The results are that the emission criterion has two regimes. When  $\gamma_s > 3\gamma_{us}$  the emission criterion is proportional to the product,  $\gamma_s\gamma_{us}$ , while when  $\gamma_s < 3\gamma_{us}$ , the criterion is proportional to  $\gamma_{us}$ . Chemical embrittlement of a crack is a direct consequence of these results, and is discussed. It is shown, however, that the localized interactions associated with chemical effects at a crack tip are inherently too complex to be encompassed in simple criteria such as these, and that quantitative predictions for chemical effects will require more detailed considerations of the specific lattice and bonding configurations in hand. But these results should serve usefully as "rule of thumb" guides.

### I. INTRODUCTION

The problem of understanding why some materials are intrinsically brittle, while others are intrinsically ductile has a long history.<sup>1-6</sup> A solid will be said to be "intrinsically" brittle when the atoms at the tip of a sharp crack can find a configuration in equilibrium between the bonding forces of the atoms at the tip which tend to close the crack, and the stress concentration caused by the external load on the solid, which tends to open the crack. If no sharp crack configuration is possible, but the cracked lattice breaks down in shear, with emission of a dislocation, then the material is intrinsically ductile. Thus, the intrinsic ductility of a material will depend on the kind of bonding forces in the solid, in addition to other factors such as the crystallography, crack plane, possible slip planes, the type of load, etc. In 1992, Rice<sup>7</sup> opened a new chapter in the history of this problem by showing that the criterion for the emission of a dislocation from a crack tip in what we will call the "Mode II configuration" is associated with the theoretical shear strength of the solid expressed as an energy—a quantity Rice called the unstable stacking fault energy,  $\gamma_{us}$ . In the Mode II configuration, the dislocation is emitted on the plane directly ahead of the crack, and the emission event does not blunt the crack tip. Zhou, Carlsson, and Thomson<sup>8</sup> (ZCT) showed that in a simple hexagonal lattice with simple force laws, for a crack in the more important "Mode I" blunting configuration (emission occurs at a nonzero angle to the crack plane), the criterion depends on a product of the unstable stacking fault energy and the intrinsic surface energy,  $\gamma_{us}\gamma_s$ . Thomson and Carlsson<sup>9</sup> attempted to understand the results of ZCT by means of standard dislocation and/or crack models, and showed that for sufficiently small surface energy, the criterion for

emission should shift from one dependent on the product,  $\gamma_s\gamma_{us}$ , to one dependent on  $\gamma_{us}$ , only.

Although the ductility criterion for bulk materials is important, fracture at various types of interfaces in materials is far more common, and this paper will address the Mode I emission criterion for cracks on interfaces. But interest in the interfacial cracking problem is high also because the elasticity analysis for that case is anomalous, and involves a singular mixing of tensile and shear modes at the tip of the crack.<sup>10,11</sup> Recently, Zhou and Thomson<sup>12</sup> addressed the emission of such a crack in the Mode II configuration, and showed that the elastic anomalies can be understood in terms of a "local core stress intensity factor." Similar ideas about cutting off the elastic solution at a critical distance in the core of the crack had been suggested earlier by Rice, Suo, and Wang.<sup>11</sup> Zhou and Thomson also showed that the Rice criterion could be applied to the interface case for the Mode II emission. In this current paper, we extend our study to the blunting Mode I interfacial configuration, with the dislocation moving into the "ductile" side of the interface couple.

As an important byproduct of this study of interfacial fracture, we shall find that the introduction of the interface also opens up the force law parameter space which can be explored, so that we can explore force laws where the arguments of Thomson and Carlsson suggest there might be a transition to the Rice type of emission criterion. Thus, the results of this study will have implications for the wider problem of intrinsic ductility in general and are not limited simply to interfacial cracking.

In the most general terms, the central problem before us is whether one can find a criterion for intrinsic ductility which can be couched in terms of simple parameters of the undeformed material such as the surface energy

and the unstable stacking fault energy. On its face, one is greatly surprised that the complex response of a material at a crack tip can be characterized by parameters which do not reflect, directly, the complicated processes acting at the crack tip. If it should turn out that such simple criteria can be found, valid for all materials and all interfaces, then one has in hand a very powerful tool for material design. It is this general question we shall address here, even though our modeling will be restricted to a simple lattice with simple force laws. If it is possible to find such criteria for our simple case, one has a powerful hint to explore for more general cases.

In the next section, we review the elastic analysis for the interface crack and present the basic equations to be used in analyzing the lattice results. In the third section, the lattice model is described, and the results are presented in the fourth section. Finally, in the fifth and sixth sections, we express our results in a form which can hopefully serve as predictive guidelines for exploring the ductility of interfaces in solids.

## II. ELASTICITY OF INTERFACIAL CRACKS

Figure 1 shows the coordinate system for a crack of length  $2a$  lying on an interface between materials 1 and 2, and emitting a dislocation at an angle  $\theta$  to the crack and interface plane. Without the dislocation, the shear stress field of the finite loaded with a point load at its center can be written<sup>11</sup>

$$\begin{aligned}\sigma_{r\theta}\sqrt{2\pi r} &= \mathcal{K}_I \Sigma_{r\theta}^I + \mathcal{K}_{II} \Sigma_{r\theta}^{II}, \\ \mathcal{K} &= \mathcal{K}_I + i\mathcal{K}_{II} = |K|e^{i(\psi-\eta)}, \\ e^{i\eta} &= \left(\frac{2a}{r}\right)^{i\epsilon}, \\ \epsilon &= \frac{1}{2\pi} \ln \frac{\kappa_1\mu_2 + \mu_1}{\kappa_2\mu_1 + \mu_2} = \frac{1}{2\pi} \ln \frac{11(c_1/c_2) + 5}{11 + 5(c_1/c_2)}.\end{aligned}\quad (1)$$

$$\begin{aligned}\Sigma_{r\theta}^I &= \frac{1}{\cosh \pi\epsilon} \left[ \sinh[(\pi - \theta)\epsilon] \sin \frac{3\theta}{2} + e^{-(\pi-\theta)\epsilon} \sin \frac{\theta}{2} \left( \cos^2 \frac{\theta}{2} - \epsilon \sin \theta \right) \right], \\ \Sigma_{r\theta}^{II} &= \frac{1}{\cosh \pi\epsilon} \left[ \cosh[(\pi - \theta)\epsilon] \cos \frac{3\theta}{2} + e^{-(\pi-\theta)\epsilon} \cos \frac{\theta}{2} \left( \sin^2 \frac{\theta}{2} + \epsilon \sin \theta \right) \right].\end{aligned}\quad (2)$$

We will interpret our lattice results in terms of the "effective  $G$ " criterion introduced by Rice for the Mode I emission in a homogeneous bulk solid.<sup>7</sup> That is, we convert the  $K$  field for the straight interface crack into the  $K$  field for a kinked crack, with the kink lying in the emission direction.<sup>13</sup> We then consider the emission process to be equivalent to the growth of the crack in the emission direction as a pure shear kink. The Mode II component of the kinking configurational force on the crack is then set equal to some lattice resistance  $\gamma$ . In Rice's formulation,  $\gamma = \gamma_{us}$ , the unstable stacking fault energy, but ZCT found that  $\gamma$  is more complicated than that. The Mode II stress intensity factor for the kinking

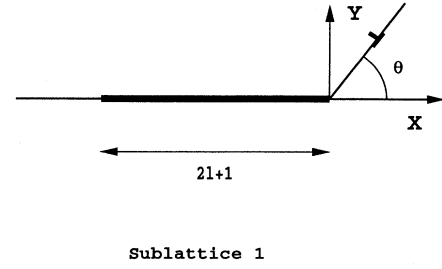


FIG. 1. A crack of length  $2a$  lying on an interface between solid 1 and solid 2. The origin of coordinates is at the right-hand tip, with the cleavage plane on the  $x$  axis. A dislocation is emitted on a slip plane intersecting the crack tip at an angle  $\theta$ . In the hexagonal lattice used,  $\theta = 60^\circ$ .

$K$  is the (complex) load stress intensity factor of the bulk material (i.e., without the interface) written as  $K = K_I + iK_{II} = |K| \exp i\psi$ , and will sometimes be referred to as the "lab" stress intensity factor.  $\psi$  is the phase angle of the load. The stress intensity factor of the interfacial crack is written as  $\mathcal{K}$  with the connection given above to the shear stress  $\sigma_{r\theta}$ . This definition for the stress intensity factor differs slightly from that in common use,<sup>11</sup> but is appropriate for the crack and load geometry in use in this work. In these equations, the additional phase angle at the crack tip generated by the elastic mismatch at the interface is given by  $\eta$ .  $\eta$  is seen to be a singular logarithmic function of the distance  $r$  from the crack tip, which is the mode mixing anomaly characteristic of interfacial cracks commented on above.  $\epsilon$  is a constant which depends on the elastic mismatch, where  $\kappa$  and  $\mu$  are the standard isotropic elastic parameters for the two materials. The expressions for  $\Sigma$  are given by<sup>11</sup>

crack in the Cotterell-Rice approximation is given by

$$\begin{aligned}k'_{II} &= \sigma_{r\theta}\sqrt{2\pi r} \\ &= \Sigma_{r\theta} K \left( \cos(\psi - \eta_e) \frac{\Sigma_{r\theta}^I}{\Sigma_{r\theta}} + \sin(\psi - \eta_e) \frac{\Sigma_{r\theta}^{II}}{\Sigma_{r\theta}} \right) \\ &= \Sigma_{r\theta} K \sin(\psi - \eta_e + \lambda_{r\theta}), \\ (\Sigma_{r\theta})^2 &= (\Sigma_{r\theta}^{II})^2 + (\Sigma_{r\theta}^I)^2, \\ \lambda_{r\theta} &= \tan^{-1}(\Sigma_{r\theta}^I/\Sigma_{r\theta}^{II}), \\ e^{i\eta_e} &= \left(\frac{2a}{r_0}\right)^{i\epsilon}.\end{aligned}\quad (3)$$

Here, we have used the idea of the “local core phase shift”  $\eta_e$  introduced by Zhou and Thomson.<sup>12</sup> That is, the phase shift at the “tip” of the crack is undefined at  $r = 0$  because of the logarithmic singularity in the definition of  $\eta$ . Thus, the appropriate phase from which to compute the kinked crack stresses is not defined. But the atomic crack has no such difficulties, because the phase in the core region of the crack, where the physics of the crack is determined, lies at some nonzero distance from the mathematical tip. Thus, we define a distance,  $r_0$  as the core size, and use that in the expressions above. (We return later to an operational definition of what to choose for  $r_0$ .) With this definition of  $r_0$ , we note that the phase  $\eta_e$  for the kinked crack does not depend on the length of the kink, because the kink lies in homogeneous material, and in this sense, the kink stress field is a “standard” crack field, not an interface field with a singular phase shift at its tip. We do have to determine what phase the kink has to start with, because it is starting out of the core of the main interface crack, but once started, the kink no longer possesses the interfacial phase anomaly as a function of its (kink) length.

According to Rice,<sup>7</sup> in terms of the kinking crack, the emission criterion  $k'_e$  for the Mode I configuration is

$$\mathcal{G}_{\text{II}e} = \frac{(k'_{\text{II}e})^2}{2\mu'_2} = \gamma. \quad (4)$$

Here,  $\mu'_2$  is the appropriate elastic modulus for the plane stress crack extension force, and  $\gamma$  is a lattice resistance, which will be determined from the lattice computations. Since the dislocation is emitted into the “ductile” side of the couple,  $\mu'_2$  must correspond to that bulk elastic parameter. (In the Rice proposal,  $\gamma = \gamma_{us}$ .) The plane stress elastic moduli are used because the two-dimensional (2D) simulations correspond to that case. Thus,  $\mu'_2 = \mu_2(1 + \nu_2)$ , where  $\mu_2$  and  $\nu_2$  are the usual plane strain elastic constants. Finally, with the previous equations, the critical load modulus  $|K|_e$  for emission is given by  $|K|_e = \sqrt{K_{\text{I}e}^2 + K_{\text{II}e}^2}$ , and

$$\mathcal{G}_{\text{II}e} = \frac{|K|_e^2}{2\mu'_2} \left( \Sigma_{r\theta}^2 \sin^2(\psi - \eta_e + \lambda_{r\theta}) \right) = \gamma. \quad (5)$$

This last equation will be used to interpret the lattice simulations. In the bulk simulations of ZCT, it was found that  $\gamma \propto \gamma_s \gamma_{us}$ , and in the current work, we will again explore the appropriate functionality for  $\gamma$ . Notice that in (5),  $\psi$  and  $\lambda_{r\theta}$  are fixed by the elastic mismatch, and by the phase of the external load.

Cleavage on the interface is governed by the simple mechanics crack extension force law,

$$\begin{aligned} \mathcal{G}_c &= \frac{K_{\text{I}}^2 + K_{\text{II}}^2}{2\mu'_{\text{eff}}} = 2\gamma_s, \\ \mu'_{\text{eff}} &= \frac{2\mu'_1\mu'_2}{\mu'_1 + \mu'_2}, \end{aligned} \quad (6)$$

where  $\mathcal{G}_c$  is the applied crack extension force, which has been found to be independent of the interface phase effects. In our atomic simulations it is always found

that the cleavage criterion is quite strictly given by the quadratic form given above. That is, the criterion is not determined primarily by the local value of  $K_{\text{I}}$ .<sup>14</sup>

The crack extension force above is written in terms of the effective force on the kinking crack. It is more natural to express it in terms of the lab stress intensity factors and lab crack forces, as

$$\begin{aligned} (\mathcal{G}_{\text{lab}})_e &= \frac{|K|_e^2}{2\mu'_2} = \frac{\gamma}{\Sigma_{r\theta}^2 \sin^2(\psi - \eta_e + \lambda_{r\theta})}, \\ |K|_e^2 &= K_{\text{I}e}^2 + K_{\text{II}e}^2. \end{aligned} \quad (7)$$

In this equation,  $(\mathcal{G}_{\text{lab}})_e$  is expressed in terms of the modulus of the loading stress intensity factor,  $|K|_e$  at the critical load when emission occurs. This form of the criterion contains, explicitly, the various factors for converting to the slip plane or kinked crack system.

A ductility parameter can be defined as the ratio of the square of the critical load stress intensity factors for cleavage and emission,

$$\begin{aligned} \mathcal{D} &= \frac{|K|_c^2}{|K|_e^2} = \frac{2\mu'_{\text{eff}} \mathcal{G}_c}{2\mu'_2 (\mathcal{G}_{\text{lab}})_e} = \frac{2\gamma_s \mu'_{\text{eff}}}{Y\gamma \mu'_2}, \\ Y &= \frac{1}{\Sigma_{r\theta}^2 \sin^2(\psi - \eta_e + \lambda_{r\theta})}, \end{aligned} \quad (8)$$

where  $\gamma$  is the effective surface energy defined by (5). The factor  $Y$  contains the kinking and interface physics. When the critical load for emission is equal to that for cleavage, and  $\mathcal{D} = 1$ , the material undergoes a crossover from ductile behavior ( $\mathcal{D} > 1$ ) to brittle behavior ( $\mathcal{D} < 1$ ). For homogeneous material,<sup>8</sup> where the misfit goes to zero, and the load is pure Mode I,  $Y(\eta_e = 0, \psi = 0, \theta = 60^\circ) = 64/9$ . Thus, the ductility parameter summarizes the crucial and complicated physics of the ductility question in a simple number. The ductility for an interface, of course, depends on the force laws to be used, as well as the load phase, elastic mismatch, and the geometry of the cleavage plane and/or slip plane.

### III. LATTICE MODEL

The lattice modeling uses the same lattice Green’s-function techniques we have used in the previous interface work,<sup>12</sup> and the general methodology is given by Thomson *et al.*<sup>15</sup> Also, we use the same 2D hexagonal lattice used previously,<sup>12,8</sup> with the same set of nearest-neighbor pair forces. It might be useful to note here that the use of the 2D lattice is not a simplification of something more general, but the 2D case is exactly the one pertaining to the physics of the problem. The reason is that we are exploring the lattice stability of the straight crack. It is true that at finite temperatures, a dislocation can be nucleated at a stable sharp crack by the generation of a dislocation loop, locally in 3D. But in the present case, we simply wish to explore the temperature-independent mechanical stability of the straight crack in the lattice, and not the ease of generation of fluctuations from that state. Thus, this is one of those rare cases in physics where the

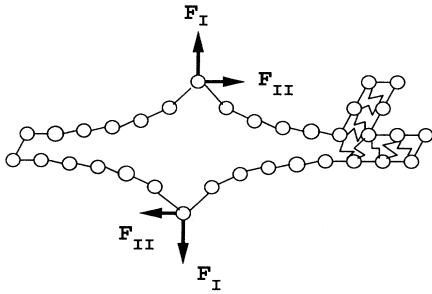


FIG. 2. The interfacial crack in a hexagonal lattice. Sublattice 1 has spring constant  $c_1$ , sublattice 2 has spring constant  $c_2 = 1$ , and the interfacial bonds have a third spring constant,  $c_{12}$ . Nonlinear bonds are formed at all atoms on the slip plane or the cleavage plane in the cohesive zone of the crack. Different nonlinear bonds can form on lower atoms, upper atoms (including the slip plane), and between atoms facing one another across the interface. The nonlinear bonds are depicted by the zig-zag lines.

simple 2D problem is precisely the one of interest. As in previous work, we also justify our use of the hexagonal lattice because it is the lattice which is isotropic in the continuum limit. Since the previous work by Rice<sup>7</sup> and the bulk of the interfacial studies are performed in the isotropic limit, we remain in that regime for the work here.

Figure 2 shows the lattice with a crack on an interface between atoms of one kind below and a second kind above. In the lattice case, we are at liberty to make the bonding between the layers different than that of either bulk, as in the real physical situation. We will arbitrarily set the elastic constant of material 2 to unity, since all the physical results scale with the elastic constant. (Of course, the ratio of the different elastic constants is a physically important quantity.) Also, we will allow the crack to emit a dislocation into only material 2, and assume that material 1 is brittle, incapable of deforming. We also make the assumption that dislocation emission takes place on the "forward" slip plane,  $\theta = 60^\circ$ , because the shear stress is largest on this plane. Subsequent emission could conceivably take place on the second slip plane,  $\theta = 120^\circ$ , but multiple emission of dislocations is not explored in this work. The crack is loaded at the center of the crack with a concentrated load. This method of loading means that the crack system is stable, because the  $K$  at the crack tip decreases as the crack length increases by the elastic equation

$$K = \frac{F_0}{\sqrt{\pi a}}, \quad (9)$$

where  $F_0$  is the point load on upper and lower crack planes, and  $a$  is the crack half length.

The present paper differs in one important respect from our earlier simulations. In this work, it is assumed that the atoms on either side of the cleavage plane and those on either side of the slip plane are in the nonlinear zone. That is, these atoms interact with all their neigh-

bors with nonlinear bonds. In previous work, only the bonds crossing the cleavage or slip plane were considered to be nonlinear, but we recently discovered that there were significant nonlinear forces acting through bonds which were assumed to be linear, so we have extended the nonlinear zone to include more bonds. Also, the atoms on the open surface are subject to a particularly subtle and important force when the surface atoms are rotated, as they are near the crack tip. Thus, the crack is always allowed to move well into the nonlinear zone to make these contributions to the crack physics negligible. When the criteria for cleavage and for emission are compared between the current method and the older one, we find that physical trends are preserved, but that small changes in critical parameters of the order of 10% are observed. These errors are not considered damaging to previous conclusions, but they are sufficiently bothersome to make the effort to reduce them further, as we have in the present paper. See the paper by Canel, Carlson, and Thomson<sup>16</sup> for further discussion of this point.

Finally, we have adopted another convention in this paper not used in the previous work. In the nonlinear zone on the crack surface, we assume that the atoms are defined to be broken up to some point about half way into the cohesive zone, and begin the cracking at this point. The physical idea is that in standard crack analysis, it is assumed that the crack is made by slitting bonds on the cleavage plane, so that a cracklike singularity can be formed at the crack tip. One needs to do that here as well, because the investigation is focused on growing cracks, not their nucleation from the perfect lattice. But in the case of the ductile lattice, there is a paradox, because no brittle crack is presumably possible. We get around this both physically and mathematically, by supposing that the brittle crack has been created by some chemical agent which acts at the growing crack tip till it reaches the size from which the computer studies begin. After the brittle crack has thus been "prepared," then the assumed bonds of the material come into play, and the crack may either cleave, or emit a dislocation. The only concern is how the core of the crack interacts with the plane on which it can emit a dislocation. In our simulations, emission on only one plane is allowed. This plane is assumed to intersect the crack tip at the exact point where the nonlinear bonds begin to act. We have also explored the effect of allowing the core to build up at the crack tip before it encounters the allowed slip plane, but this introduces only minor effects. Thus the results are quoted for the physical case shown in the figure.

As in previous work, our simulations are for a bimaterial slab. The slab is  $2 \times 10^3$  atoms thick, with the interface running down the center. The slab has periodic boundary conditions in the lateral direction, again with repeat distance of  $2 \times 10^3$  atom spacings. The crack itself is 201 atom spacings in total length, the cohesive zone is 12 atom spacings long on the cleavage plane to the right, and the inclined slip plane is 16 atom spacings long. Thus we have no worries about short crack effects, or interactions with neighboring cracks in the repeating cells, or with the free surfaces.

Once the Green's function for the cracked lattice with

interface is found,<sup>15</sup> then the displacement field for the cracked lattice in the linear approximation is given by the “master” equation for the Green’s function,

$$\mathbf{u} = \mathbf{G}\mathbf{f}. \quad (10)$$

If now one recognizes that there are given external forces  $F_0$  as well as nonlinear forces acting at bonds stretched into their nonlinear regimes, then these nonlinear forces can be treated, mathematically, as external forces, so long as the forces at these atoms are consistent with the bond stretch (or in general, with the configuration of the atom and its neighborhood). Thus one can write

$$\mathbf{u}(\mathbf{l}) = \mathbf{G}[\mathbf{F}_0 + \mathbf{f}\{\mathbf{u}(\mathbf{l})\}], \quad (11)$$

where  $\mathbf{f}\{\mathbf{u}(\mathbf{l})\}$  is the force on the atom at position  $\mathbf{l}$  considered as a functional of that position. This is a set of nonlinear equations to be solved for the set of atoms having nonlinear bonds—what we term the cohesive zone of the crack, to be solved self-consistently with the force laws assumed to be operating in the solid. Use will be made here of the simplest form of these force laws, nearest-neighbor central forces, but the formalism is quite general. These equations may be solved either by a simple relaxation program using (11) directly, or by use of a more efficient energy technique.<sup>16</sup> The methodology is accurate, provided the linear part of the lattice outside the cohesive zone is only subjected to small scale shear or to small rotations. (See Ref. 16 for further discussion of these restrictions.)

Two kinds of force law are used. The first is the universal binding relation (UBER) of Rose, Smith, and Ferrante<sup>17</sup> derived from the energy expression,

$$E(u) = c(1 - u/\alpha)e^{-u/\alpha}, \quad (12)$$

$c$  is the lattice spring constant,  $u$  is the displacement from the equilibrium distance between two atoms, and  $\alpha$  is the range parameter. The second bonding law is a Gaussian generalization of the UBER,

$$E(u) = -\frac{c\beta}{2}e^{-u^2/\beta}, \quad (13)$$

where  $\beta$  is the range parameter. (In actual practice, this law is too soft in repulsion, and a UBER form of law is welded smoothly onto it for repulsion displacements.)

#### IV. COMPUTER RESULTS

In the computer simulations, we search for stable configurations of the crack just before it cleaves on the interface, or just before it emits a dislocation on the inclined slip plane. The loads are some combination of tension (Mode I) and shear forces (Mode II) exerted to the crack surfaces at the center of the actually open crack plane. The effective load stress intensity factor  $K$  with its associated phase angle  $\psi$  can be measured by using the magnitudes of the applied forces at the critical equilibrium, and the length of the crack from (9). Figure 3 shows a typical result for the atoms of the cohesive zone

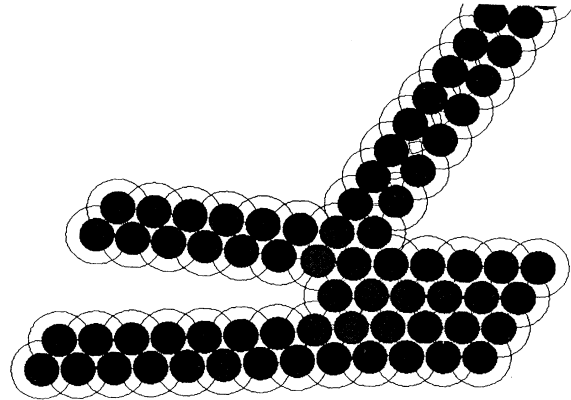


FIG. 3. Computer solution for a crack which has just emitted a dislocation on the inclined slip plane and become blunted by one lattice spacing. The crack was loaded at the center of the cleavage plane over which the bonds are completely broken. The degree of shade indicates the force on an atom exerted across the cleavage plane.

of the crack plus its slip plane.

There are four different paths the crack process can take. The crack can cleave on the original cleavage plane. It can emit a dislocation on either the interface plane or the inclined plane. And the crack can kink or branch onto the inclined plane as a cleavage crack. Under certain conditions of loading, primarily for relatively large amounts of shear, emission will take place ahead of the crack on the cleavage plane. This case is not explored here, and if the shear load is modest, then such emission does not occur. (See the previous paper by Zhou and Thomson.<sup>12</sup>) For certain force laws and loading combinations, the crack will form a kink, and cleave on the inclined plane. Again, the branching case is not studied here, but will be the subject of a later paper. The two cases studied here are emission on the inclined plane and cleavage on the initial plane, which address the issue of cleavage vs shear break down of the tip of the crack with blunting of the tip.

Simulations for three different values of the elastic mismatch,  $c_1 = 10$ ,  $c_1 = 2$ , and  $c_1 = 1$ , are carried out. The first choice represents quite an extreme value of mismatch, the second moderate mismatch, and the third represents zero mismatch. In each case, different range parameters for region 1, region 2, and for the interfacial connecting bonds between crystal blocks 1 and 2 are assumed. The range and spring constant parameters in region 2 determine the unstable stacking fault,  $\gamma_{us}$  in that region and the parameters for the connecting bonds in the interface determine the interface energy  $\gamma_s$ . The range parameter for material 1 is less important, and was chosen to be a nominal value. The spring constant in region 2 is normalized to be unity throughout. The reader will note that for the case where  $c_1 = 1$ , the material is not necessarily homogeneous, because the range parameters of the atoms at the interface and those on either side may be quite different. That is, such a case corresponds to a kind of degenerate grain boundary with a different chemical species segregated there. Although the spring

constant of the interface connecting bonds is at our disposal, we set this spring constant arbitrarily equal to unity so that  $c_2 = c_{12} = 1$ . Physically, there is no reason to do this, as  $c_{12}$  will in general be different from either bulk material, but we found that varying this parameter did not have a strong effect on the results, independent of  $\gamma_s$ .

It is clear that in the interface modeling, a wide range of parameter space is available for exploration. There is the elastic mismatch, and the three bond range parameters which can all be varied at will. In the context of the earlier work, our focus is on the two parameters,  $\gamma_s$  and  $\gamma_{us}$ . But clearly, in the modeling, we have five independent material parameters at our disposal, as well as the phase  $\psi$  of the load, so the problem is over determined in this sense. Reversing the argument, the question is whether the physical behavior is determined by only two parameters,  $\gamma_s$  and  $\gamma_{us}$ , and that is the question to which we now turn.

First, however, we note that the natural units are to take both the lattice parameter and a spring constant to unity. As noted above,  $c_2 = 1$ . In these units, and this lattice,  $\nu = 1/4$  and  $\mu = \sqrt{3}c/4$ .

### A. Core phase shift

It was explained in Sec. II that  $\eta$  was a core parameter to be determined from the atomic simulations. There are several ways to address this question. Rice, Suo, and Wang<sup>11</sup> simply assume a cutoff at the lattice parameter in the elastic equations. However, with the results of the simulations in hand, other options exist, because one can actually try to measure the phase shift in the core, and hence calculate the correct cutoff from (3). This is the approach taken in the earlier Mode II paper on interfaces.<sup>12</sup> In the present case, we can do this either on the inclined plane or on the cleavage plane. Unfortunately, we found that there was no clear way to infer the elastic core phase from the actual configurations because of various nonlinear interactions in the actual core, which go beyond the elastic picture.

Our best explanation for this failure is to note that the phase shift is an elastic concept. It will be affected by the actual nonlinearities which the crack configuration generates. If the crack opening behind the crack is sufficiently large, then the core on the inclined plane will reflect this opening, in a way not anticipated by the elastic solution. For this reason, it would be wrong to measure the core phase in the inclined plane, and infer  $r_0$  in (3) from it. In addition, when the core phase is measured on the cleavage plane, there will be elastic dislocation shielding effects from nonlinearities occurring in the inclined plane, which will alter the observed shear in the cleavage plane core. So there is little in the actual core structures which accurately reflects the elastic prediction for the phase. Nonetheless, the actual cores do exhibit the predicted phase shifts in a qualitative way, in the sense that shear loadings are certainly induced by the elastic mismatch, especially when the lattice mismatch is large enough not to be masked by core nonlinearities.

In particular, when  $c_1/c_2 = 10$ , the phase in the cleavage plane core is not swamped by the shielding in the inclined plane if the shear in that plane is not allowed to grow too large by controlling the loads on the crack. In this case, we could get quantitative measures of the core shift, which will be used in the discussion of crack length scaling effects. But for moderate values of elastic mismatch, any attempt to measure the core phase is doomed to failure, because of the interactions between the different contributions to the nonlinear core configuration.

What can one do? We remember that the purpose of this work is to see to what extent one can understand the actual crack in terms of elastic concepts, and the various lattice breakdown energies. We have argued that the phase shift which appears in the elastic analysis for the emission criterion should be measured at the core radius, as a cutoff for the elastic theory, suggesting that some version of the Rice, Suo, and Wang<sup>11</sup> approach might be appropriate. In our simulations, we find that the actual phase shifts in the cores, when they can be measured, are force law dependent. So we have adopted an empirical rule to set the core size in (3) equal to the range parameter,  $\alpha$ , in the Uber force law. In the Gaussian force law, we set  $r_0 = \sqrt{\beta}$ , because  $\sqrt{\beta}$  has the dimensions of length. The efficacy of this rule will be demonstrated entirely on the basis of its utility in comparing elastic predictions with simulation results.

### B. Emission variation with interface bonding

The principle results are shown in the following figures. Figure 4 shows the critical emission  $\mathcal{G}_{IIe}$  for a fixed value of the unstable stacking fault,  $\gamma_{us} = 0.0116$  in the normalized units of the simulation. This choice represents a relatively weak material above the interface, corresponding to the ductile material above the interface, and brittle material below. There are six series of plots, one for each choice of elastic mismatch, and one for each type of force law. For a given choice of force law type and elastic mismatch, the range parameter in the interfacial connecting bond was varied to get a range of values of  $\gamma_s$ . Figure 4 shows  $\mathcal{G}_{IIe}$  plotted against  $\gamma_s$  for each case. At the lower limiting value for  $\gamma_s$ , cleavage on the interface intervenes, and emission does not occur for any combination of loads. The upper limit is set by the fact that the range parameter becomes so short that the hexagonal lattice is no longer stable under shear load.

The plot shows a fairly narrow band of points with a linear slope. That is, all the various cases are represented by a single linear functionality in  $\gamma_s$ , which must be considered remarkable in view of all the variables which condense onto this one. But there is an interesting detail in this plot which goes beyond the linearity in  $\gamma_s$ . That is, there is a clear lower plateau in several of the plots. Further, these plateaus are all at roughly the same limiting value of 0.01, which is also roughly the value of the unstable stacking fault used in the simulations ( $\gamma_{us} = 0.0116$ ).

The first comment about these results is that our rule to set the core radius  $r_0$  to the range parameter in the

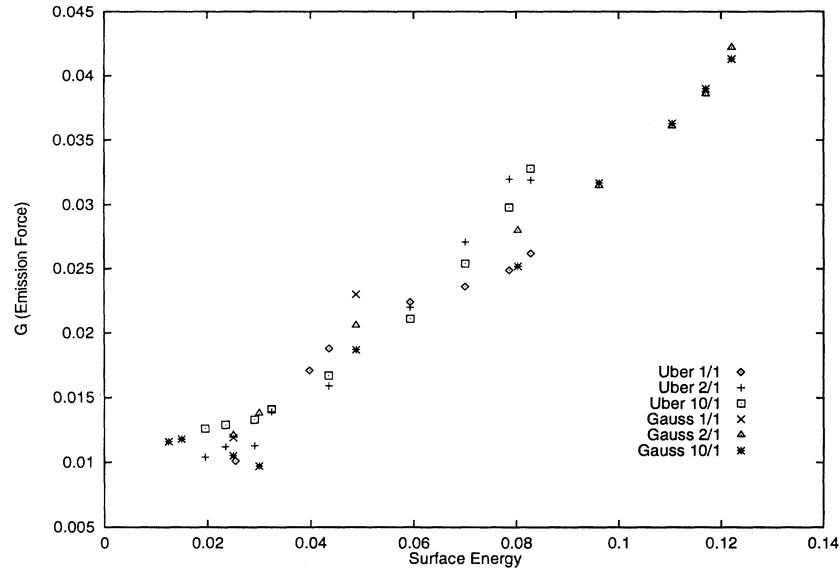


FIG. 4. Results for a series of simulations with different force laws and different elastic mismatches, when the unstable stacking fault in solid 2 is held constant at 0.0116 in the natural units of the simulation. Thus, the force law in solid 2 is held constant, and the force law on the interface is varied. However, in all cases, the spring constants are determined by the assumption made for the elastic mismatch given. We always assumed that the spring constants for the interface were the same as in solid 2. Results are shown for the effective configuration force to form the dislocation,  $\mathcal{G}_{IIe}$ , as defined in the text. Plots are separately shown for three different elastic mismatch choices, and for two different forms for the force laws. The upper limit in the plot is obtained when the force law is so long ranged that the lattice is unstable under shear, and the lower limit occurs at values of  $\gamma_s$  where the lattice cannot emit a dislocation, but can only cleave on the original cleavage plane.

force law appears to be an excellent way to calculate core phase shift effects.

Second, these results are consistent with the findings of ZCT (Ref. 8) in the homogeneous case, and are also consistent with the prediction of Thomson and Carlsson<sup>9</sup> that the emission criterion for low values of  $\gamma_s$  reverts to the Rice form. However, the functionality observed in Fig. 4 is not quantitatively that predicted by Thom-

son and Carlsson.<sup>9</sup> Those authors predict a linear law, crossing the  $\mathcal{G}_{IIe}$  axis at a finite intercept,  $\gamma_{us}$ , such that  $\mathcal{G}_{IIe} = \gamma_{us}(1 + A\gamma_s)$ , where  $A$  is a number which may depend on the elastic constants. That is, the lower shelf or plateau is not predicted by Thomson and Carlsson,<sup>9</sup> even though a limiting value of  $\mathcal{G}_{IIe}$  is. But the plateau values of  $\mathcal{G}_{us}$  fall in the range of  $\gamma_{us} = 0.0116$ , which is the intercept value from Thomson and Carlsson. Thus,

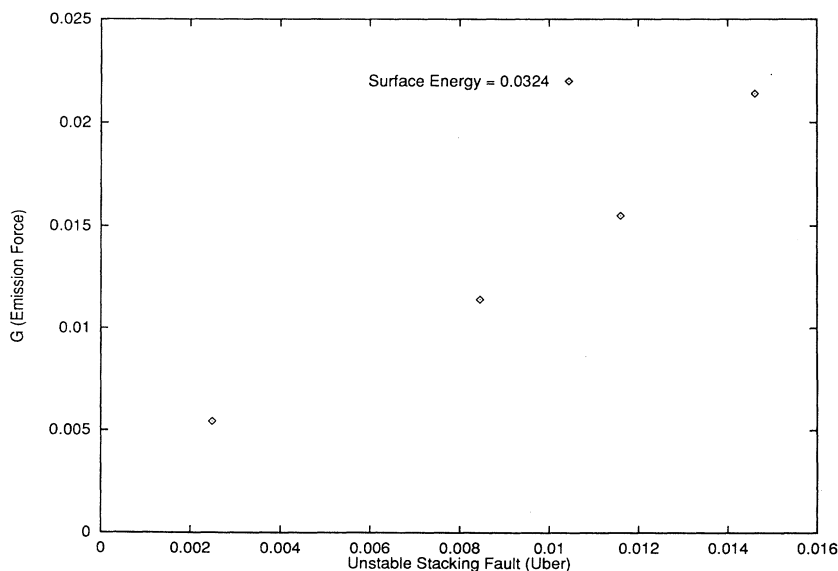


FIG. 5. Complementary results for the case where the interface bonding and  $\gamma_s$  are held constant at the "low" value of  $\gamma_s = 0.0324$  in the normalized units, and the bonding along the slip plane and  $\gamma_{us}$  is varied.

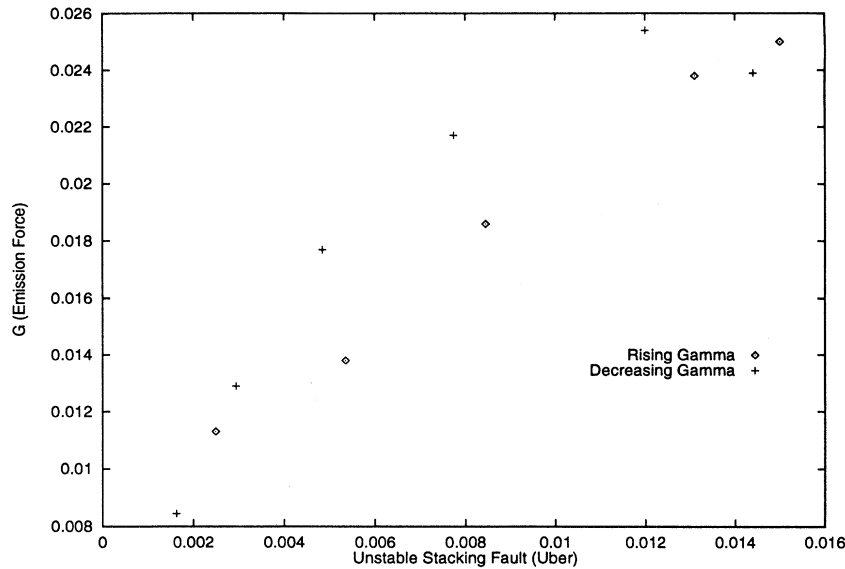


FIG. 6. Another complementary plot for the case where  $\gamma_{us}$  is varied, this time for a value of  $\gamma_s$  in the region of Fig. 5 where the plot is linear.  $\gamma_s = 0.0593$  in the normalized units. The plot shows a "hysteretic" behavior with a double valued functionality in the mid range.

Fig. 4 gives support to the general ideas expressed in the work of ZCT (Ref. 8) and Thomson and Carlsson,<sup>9</sup> even though their predictions are not borne out, quantitatively.

### C. Variation of emission with unstable stacking fault

The functionality for  $\gamma_{us}$  can also be linked to the Thomson-Carlsson form.<sup>9</sup> Two plots are displayed for  $G_{IIe}$  as a function of  $\gamma_{us}$  for fixed  $\gamma_s$ . In Fig. 5, results are shown for  $\gamma_s$  in the range of the lower shelf of Fig. 4 for the case of UBER with an elastic mismatch of 2/1. It shows a roughly linear dependence, although there is an apparent nonzero intercept for  $\gamma_{us} = 0$ , a nonphysical result. But the rough dependence is linear, as proposed

by Rice<sup>7</sup> and by Thomson and Carlsson.<sup>9</sup> A more interesting case is shown in Fig. 6, where  $G_{IIe}$  is plotted as a function of  $\gamma_{us}$  at a value of  $\gamma_s$  in the middle of the linear range of Fig. 4 for the elastic mismatch 2/1. For "rising" values of  $\gamma_{us}$ , the plot is again nicely linear, in accord with Thomson and Carlsson, however, for "decreasing" values of  $\gamma_{us}$ , there is a kind of hysteresis, and the emission function is not a unique single valued function of  $\gamma_{us}$ . The terms "rising" and "decreasing" relate to the form of the unstable stacking fault function. Figure 7 shows the unstable stacking fault function for UBER as a function of the range parameter  $\alpha$ . This function rises sharply for small values of  $\alpha$ , goes through a maximum and decays slowly back to zero for large values of  $\alpha$ . The "rising" points in Fig. 6 correspond to the values of  $\alpha$  to the left of the maximum, while the "decreasing" points

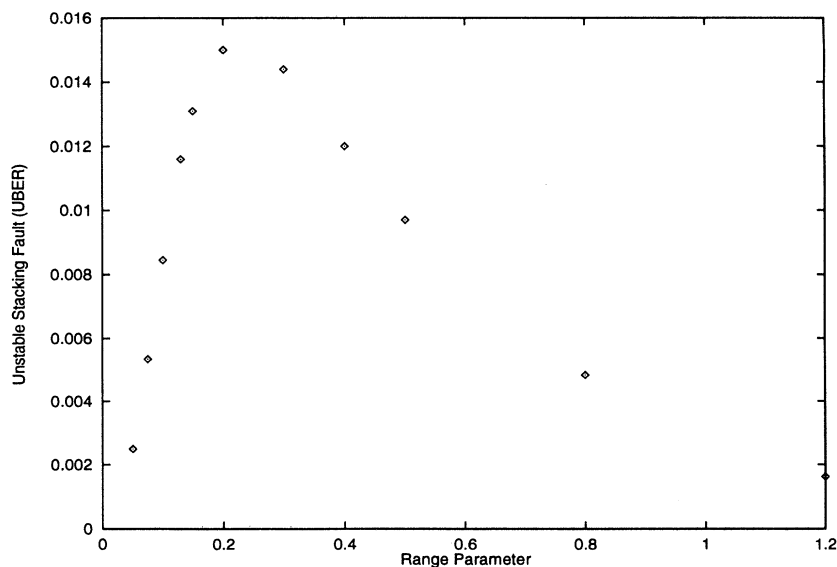


FIG. 7. Plot of the unstable stacking fault,  $\gamma_{us}$ , as a function of the range,  $\alpha$  in the UBER force law. The unstable stacking fault is the maximum energy to shear two blocks of material rigidly past one another. During the shear, the two blocks are allowed to relax in the direction normal to the slip plane.  $\gamma_{us}$  rises quickly to a maximum value and then declines for longer ranges. The points to the left of the maximum correspond to the "rising points" of the previous figure, and those to the right correspond to the "decreasing points."

correspond to the values of  $\alpha$  to the right of the maximum. The hysteretic behavior occurs in the middle of the plot, and shows a maximum deviation from a linear law of about 1.4.

#### D. Crack length scaling

With the empirical rule adopted to determine the core phase shift, it is important to check the extent to which the core phase actually corresponds to physical reality. We have commented on the fact that the cores do visually exhibit mode shifts, even though we have not been able to use a measured value of  $r_0$  in our interpretations. There is one important physical prediction which the elastic theory makes regarding to the phase shifts which must be valid for the actual simulated cracks, and that is the scaling of the phase shift in the core with the crack length, from (3). We have noted that the core phases can be reasonably well measured for large elastic mismatch, and for this case, we have investigated the scaling law.

For this exercise, we use  $c_1/c_2 = 10$  in the Uber force law, and measure the value for  $r_0$  in the cleavage plane core. We do this by finding the load which makes the shear in the core zero as measured in the simulation, and then set  $k'_{II} = 0$  in (3). For this case,  $\theta = \lambda_{r\theta} = 0$ , and the condition we seek is for the sine to be zero, or  $\eta = \psi$ . That is, the load phase is also the core phase. This computation is performed for several crack lengths, and if the core phase shift angle is a physically valid concept, then  $r_0$  should be independent of the crack length.

Figure 8 is a plot of the measured core size for the largest range of crack lengths which are possible in our computer, remembering that very short cracks will not be a fair test of the elastic theory. The simulation was done with the UBER force law, with  $\gamma_s = 0.0291$  on the interface, and with the unstable stacking fault in material 2  $\gamma_{us} = 0.0116$ . Certainly for this case, at least, crack length scaling of the core phase is excellent until short cracks are encountered.

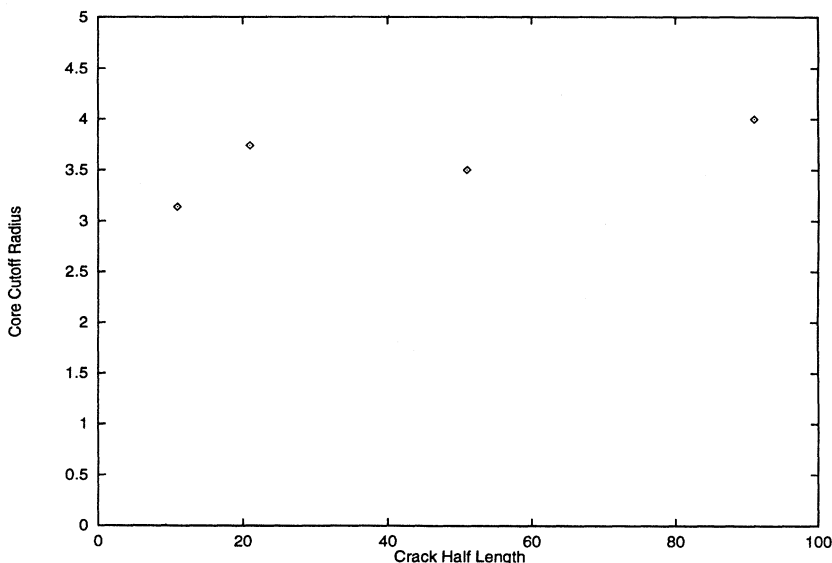


FIG. 8. Crack length scaling. The figure shows how the calculated value of the cutoff,  $r_0$  in Eq. (3) varies with the crack length.  $r_0$  should be a constant, independent of the crack length, if the underlying physics is followed. The result shows that only the shortest crack deviates sensibly from the long crack value of about 2.4.

#### V. CONCLUSIONS AND INTERPRETATION

We believe the model of Thomson and Carlsson<sup>9</sup> provides a reasonable physical basis for the cleavage and/or emission competition, when the model is extended to incorporate the observed "lower shelf" of Fig. 4. Of course, the model is only an approximation (e.g., the hysteresis of Fig. 6 is not explained), but we will show that it can form the basis for a discussion of trends, and as a kind of "rule of thumb" even for more realistic materials than are covered here. Specifically, it is possible to incorporate the entire set of simulation results from Figs. 4–6 into a single emission criterion, which is an extension of the form proposed by Thomson and Carlsson. This equation, expressed for the two separate low and high  $\gamma_s$  regimes, is

$$\begin{aligned} \mathcal{G}_{IIe} = \gamma &= \gamma_{us} \left( 0.43 + \frac{8\gamma_s}{\mu_2 b} \right); & \frac{\gamma_s}{\gamma_{us}} > 3 \\ \mathcal{G}_{IIe} = \gamma &= \gamma_{us}; & \frac{\gamma_s}{\gamma_{us}} < 3, \end{aligned} \quad (14)$$

where  $\gamma$  is the generic lattice resistance defined in (5). The first equation represents the main series of results shown in Fig. 4 where the emission is linear in  $\gamma_s$ , while the second represents the lower shelf regime. Note that the second equation can be written as a pure Rice type of criterion with no empirical factors, because all the lower plateaus level off at the observed  $\gamma_{us}$ . The first of these equations has precisely the form proposed by Thomson and Carlsson, except that the intercept is not at the  $\gamma_{us}$  value. Instead,  $\gamma_{us}$  appears as the asymptotic position for the shelf.

These equations can be expressed in terms of the crossover parameter  $\mathcal{D}$  of Eq. (8). For high values of  $\gamma_s$ , the ductility parameter has the form

$$\mathcal{D} = \frac{1}{4Y} \frac{\mu_2 b}{\gamma_{us}} \frac{\mu'_{eff}}{\mu'_2}; \quad \frac{\gamma_s}{\gamma_{us}} > 3. \quad (15)$$

TABLE I. Comparison of the effective interfacial surface energy, as calculated from the last points plotted (to the left) in Fig. 4, where the emission terminates and cleavage takes over, with the bond strength of the force law used.

$c_1/c_2$	Force law	$\mathcal{G}_c$	$2\gamma_s$
1/1	UBER	0.065	0.05
2/1	UBER	0.054	0.039
10/1	UBER	0.052	0.039
1/1	Gauss	0.059	0.05
2/1	Gauss	0.051	0.05
10/1	Gauss	0.033	0.025

This equation predicts the anomalous result, observed by ZCT,<sup>8</sup> that the ductility is independent of  $\gamma_s$ , and only depends on  $\gamma_{us}$ . That is, the crossover,  $\mathcal{D} = 1$ , occurs at a critical value of  $\gamma_{us}$ . Thus, high dislocation mobility and crack ductility go hand in hand. This result is not due to any mechanistic connection between dislocation mobility and the intrinsic ductility of the material, but rather to the fact that the same parameters of the force law control both the ductility crossover and the dislocation mobility.

In the shelf regime of the criterion, where  $\gamma_s$  is low, the ductility parameter takes the more expected form,

$$\mathcal{D} = \frac{1}{Y} \frac{2\gamma_s}{\gamma_{us}} \frac{\mu'_{\text{eff}}}{\mu_2}; \quad \frac{\gamma_s}{\gamma_{us}} < 3. \quad (16)$$

Although these criteria are constructed directly from the simulation results, a separate and partially independent check can be performed by comparing the observed left hand limiting points of the curves of Fig. 4, where cleavage takes over from emission, with the computed values of cleavage from the Griffith relation. This check is displayed in Table I, where the results are deemed to be satisfactory. Parenthetically, we note that the crossover in the simulations also exhibit the shifts which the elastic mismatch ratio in (15) and (16) predict. That is, increasing the elastic mismatch at the interface drives the material into the brittle direction.

The most important implication of Eq. (15) is that the ductile and/or brittle crossover is independent of  $\gamma_s$  in the high  $\gamma_s$  regime. This result has already been observed in the earlier work of ZCT, for the completely homogeneous case, and it is instructive to compare their results with the current case. As noted earlier, the difference between the present work and ZCT is that when  $c_1/c_2 = 1$ , and the elastic mismatch disappears in Fig. 4, there is still a bonding discontinuity at the “interface,” because the bonds at the interface are stronger than those of the matrix on either side. When there is zero elastic mismatch,  $\eta_e = 0$ , and in pure Mode I loading with  $\psi = 0$ , then for  $\theta = 60^\circ$ ,  $Y = 64/9$ . Setting  $\mathcal{D} = 1$  to find the condition for the brittle and/or ductile crossover,  $\gamma_{us}/(\mu_2 b) \simeq 0.035$  from (15), whereas ZCT obtained 0.012 for the crossover critical value.

This result shows that having a bonding inhomogeneity in the lattice does change the ductility crossover criterion significantly from the truly homogeneous case. The criterion is shifted in the ductile direction by the presence of the chemical inhomogeneity. That is, the chemically inhomogeneous material is more ductile than predicted by

ZCT in the homogeneous lattice. For the opposite case where the bonds in the interface are weaker, we would expect the shift to be opposite of that above so that the material would be more brittle than the homogeneous results predict.

The major consequence of the deviation from ZCT is that chemical embrittlement is a subtle effect which goes well beyond the ability of simple rules such as Eqs. (15) and (16) to describe completely. The physical reason is that the emission criterion and ductility parameter must be sensitive to the range (and form) of the bonding force laws in the vicinity of the interface. This follows from Thomson and Carlsson’s model of the ledge contribution when the crack is blunted. In their model, the lattice resistance is composed of a conventional unstable stacking fault term of the Rice form, and a second term arising from a correction due to the ledge energy. The ledge correction term contains the ledge surface energy  $\gamma_s$ , averaged over a suitable number of bonds as the ledge is created, multiplied by a factor which arises from the localization of the emerging dislocation density in the core. In their paper, Thomson and Carlsson calculate the localization from a Peierls dislocation model, which brings in the shear bonding between lattice planes in the form of  $\gamma_{us}$ . Both of these factors in the ledge correction term obviously depend on the range and form of the force laws. In the nearest-neighbor forces used in the current work, as well as by Thomson and Carlsson and ZCT, the ledge energy is averaged over two bonds crossing the cleavage plane. Thus, when a localized layer of strong bonds exists, as in the current work, both the averaging over the ledge energy, and the localization of the emerging dislocation core will depend on the type, form, and range of the force law used, and, in general, will lead to results different from the homogeneous solid.

Indeed, this argument shows that the criterion for ductility involves a considerable subtlety when it comes to judging how important the ledge term is in comparison to the standard Rice  $\gamma_{us}$  term in the emission criterion. When the force law has the pair form and is cut off at the second neighbor distance, as in the current work and that of ZCT, the ledge correction term is probably maximized. For example, in metals where the opening of the ledge during cleavage involves a geometry where the many-body character of the force law would lead to a weak debonding during the formation of a single step from a pure cleavage crack, the ledge term should be smaller than we have estimated. Thus, the issue of how important the ledge term is, will be one which should only be answered in the context of a full simulation of the physical geometry of the cracking lattice, with appropriate force laws.

Nevertheless, keeping in mind these provisos and warnings, the general picture we have developed on the basis of the Thomson-Carlsson physical model should provide one with considerable insight into the factors which control the intrinsic ductile and/or brittle criterion in a material. There should always be a term associated with the theoretical shear strength of the solid ( $\gamma_{us}$ ), and a term associated with the ledge formation. Although Rice and his co-workers have devoted considerable attention to the

possible importance of the tension and/or shear coupling in the  $\gamma_{us}$  part of the criterion, we have found that the simpler unvarnished (but relaxed)  $\gamma_{us}$  describes the results for the set of force laws and lattices we have used. On the basis of the Thomson-Carlsson model, and on the basis of the simulations done here and by ZCT, the ledge term appears to be composed of a product of both  $\gamma_s$  and  $\gamma_{us}$ . But we believe that even if this functionality is preserved for more realistic bonding and lattices, the relative magnitudes of the pure unstable stacking fault term and the ledge correction term will depend on the type of bonding. Thus, trends may be discernible from our results, which are probably applicable to real materials, but quantitative predictions are probably not justified, at least for chemical embrittlement situations.

In spite of these provisos and warnings, it will always be true that cleavage on the interface is governed by the Griffith condition with the interface  $\gamma_s$ , so that weakening the bonding at the interface will always enhance failure on the interface. But it need not be a brittle failure, unless  $\mathcal{D} < 1$ . Likewise, a strong matrix will always tend to suppress dislocation emission through the  $\gamma_{us}$  parameter.

To summarize our general conclusions with a “rule of thumb” statement which we believe will survive more extensive investigation: Eqs. (15) and (16) predict two regimes of behavior, and only in the case of low interfa-

cial bonding, will embrittlement be induced by a simple lowering of  $\gamma_s$ . In general, the behavior will be more complex (and interesting) than that. Exactly what “low” and “high” mean quantitatively, must be left for more realistic modeling.

We have learned that the purely interfacial effects from the lattice mismatch can be incorporated into the standard elastic descriptions of interfacial cracks, provided a core phase angle and core stress intensity factor are defined using the range of the force law as the core size.

To return to the question asked at the beginning of this paper, “Can ductility in a material be determined in terms of bulk material parameters?,” the answer is only provisionally “yes”—if trends and qualitative features are desired. But localized chemical embrittlement, such as occurs during segregation at an interface, appears to require a full crack simulation for definitive answers.

#### ACKNOWLEDGMENTS

It is a pleasure to acknowledge discussion and help on this work from my colleagues, Anders Carlsson, Lilly Canel, and Jakob Schiotz, all of the University of Washington, St. Louis. Early stages of the work were supported in part by the ONR (N00014-92-F-0098). The main effort was supported by NIST, formerly as employer, and lately under grant to Washington University.

- 
- <sup>1</sup> R. Armstrong, *Mater. Sci. Eng.* **1**, 251 (1966).  
<sup>2</sup> A. Kelly, W. Tyson, and A. H. Cottrell, *Philos. Mag.* **15**, 567 (1967).  
<sup>3</sup> J. R. Rice and R. Thomson, *Philos. Mag.* **29**, 73 (1974).  
<sup>4</sup> J. Weertman, *Philos. Mag.* **43**, 1103 (1981).  
<sup>5</sup> G. Schoeck, *Philos. Mag.* **63**, 111 (1991).  
<sup>6</sup> G. Schoeck, *J. Mech. Phys. Solids* (to be published).  
<sup>7</sup> J. R. Rice, *J. Mech. Phys. Solids* **40**, 239 (1992).  
<sup>8</sup> S. J. Zhou, A. Carlsson, and R. Thomson, *Phys. Rev. Lett.* **72**, 852 (1994).  
<sup>9</sup> R. Thomson and A. Carlsson, *Philos. Mag.* **70**, 893 (1994).  
<sup>10</sup> M. L. Williams, *Bull. Seismol. Soc. Am.* **49**, 199 (1959); A. H. England, *J. Appl. Mech.* **32**, 400 (1965); J. W. Hutchinson, M. E. Mear, and J. R. Rice, *ibid.* **54**, 828 (1987).  
<sup>11</sup> J. R. Rice, Z. Suo, and J.-S. Wang, in *Metal-Ceramics Interfaces*, edited by M. Ruhle, A. G. Evans, M. F. Ashby, and J. Hirth, *Acta Scripta Met. Proceedings Series 4* (Pergamon, New York, 1990), p. 269.  
<sup>12</sup> S. J. Zhou and R. Thomson, *Phys. Rev. B* **49**, 44 (1994).  
<sup>13</sup> B. Cotterell and J. R. Rice, *Int. J. Fract.* **16**, 155 (1980).  
<sup>14</sup> R. Thomson, *J. Phys. Chem. Solids* **55**, 1165 (1994).  
<sup>15</sup> R. Thomson, S. J. Zhou, A. Carlsson, and V. Tewary, *Phys. Rev. B* **46**, 10 613 (1992).  
<sup>16</sup> L. Canel, A. Carlsson, and R. Thomson, *Phys. Rev. B* **52**, 158 (1995).  
<sup>17</sup> J. Rose, J. Smith, and J. Ferrante, *Phys. Rev.* **28**, 1835 (1983).